

QUASILINEAR DRIFT OF COSMIC RAYS IN WEAK TURBULENT ELECTROMAGNETIC FIELDS

Olaf Stawicki

*Unit for Space Physics, North-West University, Potchefstroom Campus, Private Bag X6001,
Potchefstroom 2520, South Africa*

fskos@puk.ac.za

ABSTRACT

A general quasilinear transport parameter for particle drift in arbitrary turbulence geometry is presented. The new drift coefficient is solely characterized by a nonresonant term and is evaluated for slab and two-dimensional turbulence geometry. The calculations presented here demonstrate that fluctuating electric fields are a key quantity for understanding quasilinear particle drift in slab geometry. It is shown that particle drift does not exist in unpolarized and purely magnetic slab fluctuations. This is in stark contrast to previous models, which are restricted to slab geometry and the field line random walk limit. The evaluation of the general transport parameter for two-dimensional turbulence geometry, presented here for the first time for dynamical magnetic turbulence, results in a drift coefficient valid for a magnetic power spectrum and turbulence decay rate varying arbitrarily in wavenumber. For a two-component, slab/two-dimensional turbulence model, numerical calculations are presented. The new quasilinear drift, induced by the magnetic perturbations, is compared with a standard drift expression related to the curvature and gradient of an unperturbed heliospheric background magnetic field. The considerations presented here offer a solid ground and natural explanation for the hitherto puzzling observation that drift models often describe observations much better when drift effects are reduced.

Subject headings: cosmic rays — drifts — turbulence

1. INTRODUCTION AND MOTIVATION

Particle transport in random magnetic fields plays a key role in space physics and astrophysics. The knowledge of turbulence properties is crucial for understanding (anisotropic) particle diffusion in a collisionless, turbulent and magnetized plasma such as the solar wind or the interstellar medium. Of particular interest are processes governing particle diffusion across an ambient magnetic field, and perpendicular diffusion and particle drifts appear to be the primary mechanisms. Transport

coefficients describing these two processes are thus key quantities for several heliospheric and astrophysical settings such as solar modulation of cosmic rays and diffusive shock acceleration, e.g., at the heliospheric shock of termination or at shocks triggered by supernovae.

It is generally accepted that the modulation of cosmic rays in the heliosphere is described adequately by Parker’s equation (Parker 1965) taking into account (anisotropic) spatial diffusion of cosmic rays by the diffusion tensor \mathbf{K} . This tensor describes the interaction of cosmic rays with the turbulence. In a local orthogonal coordinate system with one axis along the direction of the mean magnetic field, it takes on its simplest form and reads

$$\mathbf{K} = \begin{pmatrix} \kappa_{\perp,1} & \kappa_A & 0 \\ -\kappa_A & \kappa_{\perp,2} & 0 \\ 0 & 0 & \kappa_{\parallel} \end{pmatrix}. \quad (1)$$

The diagonal elements describe diffusion along (κ_{\parallel}) and perpendicular ($\kappa_{\perp,1}$, $\kappa_{\perp,2}$) to the mean magnetic field. The off-diagonal, antisymmetric entry κ_A is related to effects of curvature and gradient drift in a nonhomogeneous heliospheric magnetic field (HMF). For an unmodified Parker spiral (Parker 1958), κ_A reads (Jokipii et al. 1977)

$$\kappa_A = \frac{vR_L}{3}, \quad (2)$$

where v and R_L denote the speed and the Larmor radius of a particle, respectively. The derivation of equation (2) is based on the assumption that the HMF is undisturbed, i.e., electromagnetic turbulent fields are not taken into account.

The importance of large-scale drifts of cosmic rays in the HMF was first recognized in the late seventies by Jokipii et al. (1977) and subsequently taken into account, via equation (2), in enumerable numerical studies (e.g., Potgieter & Burger 1990; Webber et al. 1990; Potgieter et al. 1993; Burger & Hattingh 1998). While being indispensable for a description of multi-dimensional large-scale modulation, it has been demonstrated that drift effects do not have to be included in all cases to reproduce observations (see, e.g., Reinecke et al. 1993; le Roux & Fichtner 1997).

It has been pointed out in several numerical studies that the effect on modulation, as described by equation (2), is too large if the numerical results are compared with observations (e.g., Potgieter et al. 1987, 1989; Potgieter & Burger 1990; Webber et al. 1990). To obtain a better agreement between simulations and observations, it was suggested to use a reduced amount of drift effects at low and intermediate particle energies (Potgieter et al. 1987, 1989; Burger 1990). In spite of its importance and the pressing need of rigorous theories, only one model has been developed in the past being able to explain a possible reduction of the drift at intermediate energies (Bieber & Matthaeus 1997). In brief, they obtain the expression

$$\kappa_A = \frac{vR_L}{3} \frac{(\tau\Omega)^2}{1 + (\tau\Omega)^2} \quad (3)$$

with Ω being the relativistic particle gyrofrequency. The timescale τ is associated with the decorrelation of a particle trajectory from an unperturbed helical orbit. For their calculations, Bieber

& Matthaeus (1997) assume slab turbulence geometry and argue that nonresonant field line random walk (FLRW) is the major agent for the decorrelation of particle trajectories. Based on this, they demonstrate that drift effects can be suppressed at low and intermediate particle energies. Another model, developed earlier by Forman et al. (1974) on the basis of quasilinear theory (QLT) and FLRW in slab geometry, is formally based on the same expression for κ_A , equation (3). It has been shown, however, that this model fails in explaining suppressed drift effects, since their approach is valid only for cosmic ray energies greater than ~ 3 GeV at Earth (Bieber & Matthaeus 1997). Besides being valid for slab geometry only, both models take into account purely magnetic fluctuations and were developed for static turbulence only. Finally, for completeness, it should be mentioned that equation (3) is formally the same as for hard-sphere scattering in a magnetized plasma (Gleeson 1969), where τ is then the scattering time. Furthermore, a similar structure was found for collisional particle transport parameter in a thermal equilibrium plasma (Balescu et al. 1994) and expressions for coefficients being of similar forms were already considered in the mid 1960s (cf., e.g., Toptygin 1985, and references therein).

Upon looking into the literature, one becomes aware of the fact that a rigorous, quasilinear treatment of particle drift in an electromagnetic plasma wave turbulence with arbitrary geometry does not exist. The purpose of this paper is, therefore, to present a solid QLT treatment of particle drift in slab and, particularly, 2D turbulence geometry.

The structure of the paper is as follows: Section 2 introduces the governing QLT equations of motions (Sec. 2.1) required for the evaluation of second-order velocity cross-correlation functions (Sec. 2.2). General Fokker-Planck coefficients and drift coefficients valid for arbitrary turbulence geometry and arbitrary plasma wave dispersion relations are presented in Sec. 2.3. Drift coefficients for an electromagnetic plasma wave turbulence with slab geometry are presented in section 3. Section 4 gives a QLT particle drift coefficient for 2D turbulence geometry, presented here for the first time. The new drift coefficient is valid for an arbitrary wavenumber dependence of the magnetic power spectrum and the turbulence decorrelation rate. Numerical calculations for a two-component turbulence model are presented, together with the conclusions, in section 5.

2. QUASILINEAR FORMALISM

Spatial diffusion and drift coefficients are commonly calculated from an ensemble of particle trajectories. For statistically homogeneous and stationary fluctuations, the so-called Taylor-Green-Kubo (TGK) formula (e.g., Kubo 1957) is often employed,

$$\kappa_{ij} = \int_0^t d\xi \langle v_i(0)v_j(\xi) \rangle, \quad (4)$$

in the limit $t \rightarrow \infty$. Here, v_i is the i th Cartesian component of the single particle velocity. The brackets $\langle \dots \rangle$ denote an ensemble average over the relevant distribution of particles. For large

coherence time ξ , the second-order velocity correlation function $\langle v_i(0)v_j(\xi) \rangle$ must go to zero, and the integral in equation (4) approaches a constant value for $t \rightarrow \infty$.

Within the context of QLT, the transport coefficients κ_{ij} can be written as (Schlickeiser 2002, Eq. (12.3.25))

$$\kappa_{ij} = \frac{1}{2} \int_{-1}^1 d\mu D_{X_i X_j}, \quad (5)$$

where $\mu = v_{\parallel}/v$ is the pitch-angle of a particle having the velocity component v_{\parallel} along the ordered magnetic field B_0 . The subscripts X_i and X_j denote guiding center coordinates in the i th and j th Cartesian direction, respectively, and $D_{X_i X_j}$ denotes Fokker-Planck coefficients of the form

$$D_{X_i X_j} = \Re \int_0^{\infty} d\xi \langle \dot{X}_i(0) \dot{X}_j^*(\xi) \rangle. \quad (6)$$

They represent the interaction of a particle with electromagnetic fluctuations. The relation in equation (6) correspond to the TGK formula (4) used earlier by Bieber & Matthaeus (1997) and Forman et al. (1974). In QLT, however, one has to perform an additional average with respect to μ .

To evaluate the QLT transport coefficients for particle drift in a large-scale magnetic field with superimposed electromagnetic fluctuations, the corresponding Fokker-Planck coefficients D_{XY} and D_{YX} have to be calculated. This requires the temporal variations of the quiding center coordinates. The particle equations of motion then enable one to calculate the corresponding second-order velocity cross-correlation functions.

2.1. EQUATIONS OF MOTION

According to Schlickeiser (2002, Eqs. (12.1.9d) and (12.1.9e)), the perpendicular components of the fluctuating force fields can be written as

$$\dot{X}(t) = -v \cos \phi(t) \sqrt{1 - \mu^2} \frac{\delta B_{\parallel}}{B_0} + \frac{c}{B_0} \left(\delta E_y + \mu \frac{v}{c} \delta B_x \right) \quad (7)$$

$$\dot{Y}(t) = -v \sin \phi(t) \sqrt{1 - \mu^2} \frac{\delta B_{\parallel}}{B_0} - \frac{c}{B_0} \left(\delta E_x - \mu \frac{v}{c} \delta B_y \right), \quad (8)$$

where ϕ and c denote the gyrophase of the particle and the speed of light, respectively. Note that the Cartesian components $\delta B_{x,y,\parallel}$ and $\delta E_{x,y,\parallel}$ of the fluctuating electromagnetic field are used and not the helical description, i.e., left- and right-hand polarized fields. For the further treatment of equations (7) and (8), a standard perturbation method is applied. To do so, it is convenient to replace in the Fourier transform of the irregular electromagnetic field the true particle orbit $\mathbf{x}(t)$

by an unperturbed particle orbit, yielding

$$\delta \mathbf{B}(\mathbf{x}, t) = \int d^3k \delta \mathbf{B}(\mathbf{k}, t) e^{i\mathbf{x}(t) \cdot \mathbf{k}} = \sum_{n=-\infty}^{+\infty} \int d^3k \delta \mathbf{B}(\mathbf{k}, t) J_n(W) \exp \left[i n [\psi - \phi(t)] + i k_{\parallel} v_{\parallel} t \right] \quad (9)$$

and an analogous expression for $\delta \mathbf{E}$. The quantity $J_n(W)$ is a Bessel function of the first kind and order n . The particle gyrophase for an unperturbed orbit is given by $\phi(t) = \phi_0 - \Omega t$, where the random variable ϕ_0 denotes the initial gyrophase of the particle. Furthermore, the abbreviation $W = k_{\perp} R_L \sqrt{1 - \mu^2}$ is introduced, where $R_L = v/\Omega$ is the Larmor radius. The relativistic gyrofrequency is given by $\Omega = qB_0/(\gamma mc)$ with m being the mass and q the charge of the particle, γ is the Lorentz factor. The angle ψ results from the wavenumber representation $k_x = k_{\perp} \cos \psi$ and $k_y = k_{\perp} \sin \psi$. With equation (9), the equations of motion (7) and (8) can be manipulated to become

$$\dot{X}(t) = \frac{v}{B_0} \sum_{n=-\infty}^{\infty} \int d^3k \exp \left[i n [\psi - \phi(t)] + i k_{\parallel} v_{\parallel} t \right] \quad (10)$$

$$\times \left\{ -\frac{\sqrt{1 - \mu^2}}{2} \left[J_{n+1}(W) e^{i\psi} + e^{-i\psi} J_{n-1}(W) \right] \delta B_{\parallel} + \frac{c}{v} J_n(W) \left(\delta E_y + \mu \frac{v}{c} \delta B_x \right) \right\}$$

$$\dot{Y}(t) = \frac{v}{B_0} \sum_{n=-\infty}^{\infty} \int d^3k \exp \left[i n [\psi - \phi(t)] + i k_{\parallel} v_{\parallel} t \right] \quad (11)$$

$$\times \left\{ i \frac{\sqrt{1 - \mu^2}}{2} \left[J_{n+1}(W) e^{i\psi} - e^{-i\psi} J_{n-1}(W) \right] \delta B_{\parallel} - \frac{c}{v} J_n(W) \left(\delta E_x - \mu \frac{v}{c} \delta B_y \right) \right\}.$$

For the evaluation of equation (5), it is convenient to consider now the nature of the electromagnetic turbulence. Here, the “plasma wave viewpoint” is employed and it is assumed that the turbulence consists of a superposition of N individual plasma wave modes, i.e.,

$$\delta \mathbf{B}(\mathbf{k}, t) = \sum_{j=1}^N \delta \mathbf{B}^j(\mathbf{k}) \exp(-i\omega_j t) ; \quad \delta \mathbf{E}(\mathbf{k}, t) = \sum_{j=1}^N \delta \mathbf{E}^j(\mathbf{k}) \exp(-i\omega_j t). \quad (12)$$

Here, $\omega_j(\mathbf{k}) = \omega_{j,R}(\mathbf{k}) + i\Gamma_j(\mathbf{k})$ is a complex dispersion relation of wave mode j , where $\omega_{j,R}$ is the real frequency of the mode. The imaginary part, $\Gamma_j(\mathbf{k}) \leq 0$, represents dissipation of turbulent energy due to plasma wave damping.

Restricting the considerations to transverse ($\delta \mathbf{E}^j \cdot \mathbf{k} = 0$) fluctuations and using Faraday’s law, the turbulent electric field can easily be expressed by the corresponding magnetic counterparts, yielding

$$\delta E_x^j = \frac{\omega_j}{ck^2} \left(\delta B_y^j k_{\parallel} - \delta B_{\parallel}^j k_y \right) ; \quad \delta E_y^j = \frac{\omega_j}{ck^2} \left(\delta B_{\parallel}^j k_x - \delta B_x^j k_{\parallel} \right). \quad (13)$$

Furthermore, it is convenient to use the Bessel function identities

$$J_{n-1}(W) + J_{n+1}(W) = \frac{2n}{W} J_n(W) ; \quad J_{n-1}(W) - J_{n+1}(W) = 2J'_n(W), \quad (14)$$

where the prime denotes the derivation with respect to W . With equations (13) and (14), Eqs. (10) and (11) can readily be rearranged to become

$$\begin{aligned} \dot{X}(t) = & -\frac{v}{B_0} \sum_j \sum_{n=-\infty}^{\infty} \int d^3k \exp \left[in [\psi - \phi(t)] + i(k_{\parallel} v_{\parallel} - \omega_j)t \right] \\ & \times \left\{ J_n(W) \left[a \frac{k_x}{k_{\perp}} \delta B_{\parallel}^j + b \delta B_x^j \right] - i \sqrt{1 - \mu^2} \frac{k_y}{k_{\perp}} \delta B_{\parallel}^j J'_n(W) \right\} \end{aligned} \quad (15)$$

$$\begin{aligned} \dot{Y}(t) = & -\frac{v}{B_0} \sum_{j=1}^N \sum_{n=-\infty}^{\infty} \int d^3k \exp \left[in [\psi - \phi(t)] + i(k_{\parallel} v_{\parallel} - \omega_j)t \right] \\ & \times \left\{ J_n(W) \left[a \frac{k_y}{k_{\perp}} \delta B_{\parallel}^j + b \delta B_y^j \right] + i \sqrt{1 - \mu^2} \frac{k_x}{k_{\perp}} \delta B_{\parallel}^j J'_n(W) \right\}, \end{aligned} \quad (16)$$

where the following complex functions have been introduced:

$$a = \frac{n}{W} \sqrt{1 - \mu^2} - \frac{\omega_j k_{\perp}}{v k^2} ; \quad b = \frac{\omega_j k_{\parallel}}{v k^2} - \mu. \quad (17)$$

2.2. VELOCITY CROSS-CORRELATION FUNCTIONS

Having determined the equations of motion, one can now proceed to calculate the second-order velocity cross-correlation functions $\langle \dot{X}(0) \dot{Y}^*(\xi) \rangle$ and $\langle \dot{Y}(0) \dot{X}^*(\xi) \rangle$ entering equation (6). The procedure for the calculation is relatively lengthy, but can be carried out with simple algebra. The calculations for both correlation functions are analogous, and the calculations are restricted to $\langle \dot{X}(0) \dot{Y}^*(\xi) \rangle$. Multiplication of equation (15) with the conjugate of equation (16) leads to

$$\begin{aligned} \dot{X}(0) \dot{Y}^*(\xi) = & \frac{v^2}{B_0^2} \sum_j \sum_{n=-\infty}^{\infty} \sum_{m=-\infty}^{\infty} \int d^3k \int d^3\bar{k} \exp(\chi) \\ & \times \left\{ J_n(W) J_m(\bar{W}) \left[\frac{k_x \bar{k}_y}{k_{\perp} \bar{k}_{\perp}} a \bar{a}^* \cdot (\delta B_{\parallel}^j \delta \bar{B}_{\parallel}^{j*}) + b \bar{b}^* \cdot (\delta B_x^j \delta \bar{B}_y^{j*}) \right. \right. \\ & \quad \left. \left. + \frac{k_x}{k_{\perp}} a \bar{b}^* \cdot (\delta B_{\parallel}^j \delta \bar{B}_y^{j*}) + \frac{\bar{k}_y}{\bar{k}_{\perp}} \bar{a}^* b \cdot (\delta B_x^j \delta \bar{B}_{\parallel}^{j*}) \right] \right. \\ & - i \sqrt{1 - \mu^2} J_m(\bar{W}) J'_n(W) \frac{k_y}{k_{\perp}} \left[\frac{\bar{k}_y}{\bar{k}_{\perp}} \bar{a}^* \cdot (\delta B_{\parallel}^j \delta \bar{B}_{\parallel}^{j*}) + \bar{b}^* \cdot (\delta B_{\parallel}^j \delta \bar{B}_y^{j*}) \right] \\ & - i \sqrt{1 - \mu^2} J_n(W) J'_m(\bar{W}) \frac{\bar{k}_x}{\bar{k}_{\perp}} \left[\frac{k_x}{k_{\perp}} a \cdot (\delta B_{\parallel}^j \delta \bar{B}_{\parallel}^{j*}) + b \cdot (\delta B_x^j \delta \bar{B}_{\parallel}^{j*}) \right] \\ & \left. - (1 - \mu^2) \frac{k_y \bar{k}_x}{k_{\perp} \bar{k}_{\perp}} J'_n(W) J'_m(\bar{W}) \cdot (\delta B_{\parallel}^j \delta \bar{B}_{\parallel}^{j*}) \right\} \end{aligned} \quad (18)$$

with $\chi = \imath(n\psi - m\bar{\psi}) - \imath(n - m)\phi_0 - \imath(\bar{k}_{\parallel}v_{\parallel} - \bar{\omega}_j^* + m\Omega)\xi$. The bar notation used over some quantities indicates that they have to be evaluated for wavevector $\bar{\mathbf{k}}$ and time ξ .

A further simplification of (18) can be achieved only if an average with respect to the random variable ϕ_0 , the initial gyrophase of the particle, is applied. For this, the relation

$$\frac{1}{2\pi} \int_0^{2\pi} d\phi_0 \exp[\imath(n - m)\phi_0] = \delta_{nm} \quad (19)$$

is used, where $\delta_{nm} = 0$ for $n \neq m$ and unity for $n = m$. Furthermore, the ensemble average is applied and it is assumed that the Fourier components at different wave vectors are uncorrelated. Introducing the subscripts α and β for Cartesian coordinates, the ensemble averages of the magnetic field fluctuations then read

$$\langle \delta B_{\alpha}^j \delta \bar{B}_{\beta}^{j*} \rangle = \langle \delta B_{\alpha}^j(\mathbf{k}) \delta B_{\beta}^{j*}(\mathbf{k}') \rangle = \delta(\mathbf{k} - \mathbf{k}') P_{\alpha\beta}^j(\mathbf{k}). \quad (20)$$

The uncorrelated state implies $\psi = \bar{\psi}$, $W = \bar{W}$ and $\omega_j = \bar{\omega}_j$. Equation (18) can then be manipulated to become

$$\begin{aligned} \langle \dot{X}(0) \dot{Y}^*(\xi) \rangle &= \frac{v^2}{B_0^2} \sum_j \sum_{n=-\infty}^{\infty} \int d^3k k_{\perp}^{-2} \exp[-\imath(k_{\parallel}v_{\parallel} - \omega_j^* + n\Omega)\xi] \\ &\times \left\{ J_n^2(W) \left[k_x k_y a a^* P_{\parallel\parallel}^j + k_{\perp}^2 b b^* P_{xy}^j + k_x k_{\perp} a b^* P_{\parallel y}^j + k_y k_{\perp} a^* b P_{x\parallel}^j \right] \right. \\ &- \imath \sqrt{1 - \mu^2} J_n(W) J'_n(W) \left[P_{\parallel\parallel}^j (k_y^2 a^* + k_x^2 a) + k_{\perp} k_y b^* P_{\parallel y}^j + k_{\perp} k_x b P_{x\parallel}^j \right] \\ &\left. - (1 - \mu^2) k_y k_x [J'_n(W)]^2 P_{\parallel\parallel}^j \right\} \end{aligned} \quad (21)$$

and an analogous expression for the cross-correlation function $\langle \dot{Y}(0) \dot{X}^*(\xi) \rangle$ governing the transport parameter κ_{YX} was derived. Both are expressed by a sum of three individual terms, and each term is accompanied by a specific factor through which the components of the magnetic correlation tensor $P_{\alpha\beta}^j(\mathbf{k}, \xi)$ enter the cross-correlation functions.

2.3. FOKKER-PLANCK COEFFICIENTS

Having determined the velocity cross-correlation for κ_{XY} in the previous section, one can now proceed and evaluate the corresponding Fokker-Planck coefficient D_{XY} . Upon substituting equation (21) into (6), one obtains

$$D_{XY} = \frac{v^2}{B_0^2} \sum_j \sum_{n=-\infty}^{\infty} \Re \int d^3k \frac{\mathcal{R}_j}{k_{\perp}^2} \left[J_n^2(W) F_{XY}^j - \imath J_n(W) J'_n(W) G_{XY}^j - [J'_n(W)]^2 H_{XY}^j \right] \quad (22)$$

with the auxiliary functions

$$F_{XY}^j = k_x k_y a a^* P_{|||}^j + k_{\perp}^2 b b^* P_{xy}^j + k_x k_{\perp} a b^* P_{||y}^j + k_y k_{\perp} a^* b P_{x||}^j \quad (23)$$

$$G_{XY}^j = \sqrt{1 - \mu^2} \left[P_{|||}^j (k_y^2 a^* + k_x^2 a) + k_{\perp} k_y b^* P_{||y}^j + k_{\perp} k_x b P_{x||}^j \right] \quad (24)$$

$$H_{XY}^j = (1 - \mu^2) k_y k_x P_{|||}^j. \quad (25)$$

The integration with respect to ξ leads to the complex resonance function,

$$\mathcal{R}_j = \int_0^{\infty} d\xi \exp \left[-\imath(k_{||} v_{||} - \omega_{j,R} + n\Omega)\xi + \Gamma_j \xi \right] = -\frac{\Gamma_j + \imath(k_{||} v_{||} - \omega_{j,R} + n\Omega)}{\Gamma_j^2 + (k_{||} v_{||} - \omega_{j,R} + n\Omega)^2} \quad (26)$$

which describes interactions of the particles with the plasma wave turbulence. The calculations for the Fokker-Planck coefficient D_{YX} are analogous to the calculations for D_{XY} and result in

$$D_{YX} = \frac{v^2}{B_0^2} \sum_j \sum_{n=-\infty}^{\infty} \Re \int d^3 k \frac{\mathcal{R}_j}{k_{\perp}^2} \left[J_n^2(W) F_{YX}^j + \imath J_n(W) J_n'(W) G_{YX}^j - [J_n'(W)]^2 H_{YX}^j \right] \quad (27)$$

with the corresponding auxiliary functions

$$F_{YX}^j = k_x k_y a a^* P_{|||}^j + k_{\perp}^2 b b^* P_{yx}^j + k_x k_{\perp} a^* b P_{y||}^j + k_y k_{\perp} a b^* P_{||x}^j \quad (28)$$

$$G_{YX}^j = \sqrt{1 - \mu^2} \left[P_{|||}^j (k_x^2 a^* + k_y^2 a) + k_{\perp} k_y b P_{y||}^j + k_{\perp} k_x b^* P_{||x}^j \right] \quad (29)$$

$$H_{YX}^j = (1 - \mu^2) k_x k_y P_{|||}^j. \quad (30)$$

Equations (22) and (27), one of the main results of this paper and presented here in this general form for the first time, allow one to calculate QLT drift coefficients for arbitrary turbulence geometry, where the turbulence consists of transverse wave modes with dispersion relations depending arbitrarily on wavevector.

Further treatment of the auxiliary functions (23) to (25) and (28) to (30) requires a certain representation for the correlation tensor $P_{\alpha\beta}^j$. Different representations for $P_{\alpha\beta}^j$ will alter the underlying mathematical and physical structure of the Fokker-Planck and, therefore, the drift coefficients. Here, a representation is chosen commonly used in the literature. Following, e.g., Lerche & Schlickeiser (2001), the nine components of $P_{\alpha\beta}^j$ can be expressed as

$$P_{\alpha\beta}^j(k_{\perp}, k_{||}) = A^j(k_{\perp}, k_{||}) \left[\delta_{\alpha\beta} - \frac{k_{\alpha} k_{\beta}}{k^2} + \imath \sigma^j(k_{\perp}, k_{||}) \epsilon_{\alpha\beta\nu} \frac{k_{\nu}}{k} \right], \quad (31)$$

where σ^j denotes the magnetic helicity, $\delta_{\alpha\beta}$ is Kronecker's delta and $\epsilon_{\alpha\beta\gamma}$ is the Levi-Civita tensor, A^j is the wave power spectrum. With equation (31), one can now proceed to evaluate the Fokker-Planck coefficients (22) and (27). The calculations are very laborious and result in quite lengthy expressions. For the sake of overview, a simplification is introduced which concerns the complex functions a and b given by equation (17). Their complex nature results from the imaginary part of the wave mode dispersion relation, i.e., the dissipation rate Γ_j . It enters a and b via Faraday's law used to express the turbulent electric field components by their magnetic counterparts. For instance, consider the first term in equations (23) and (28). The quantity aa^* can also be written as

$$aa^* = \left(\frac{n}{W} \sqrt{1 - \mu^2} - \frac{\omega_{j,R} k_\perp}{v k^2} \right)^2 + \frac{\Gamma_j k_\perp^2}{v^2 k^4} = a_R^2 + \frac{\Gamma_j k_\perp^2}{v^2 k^4}. \quad (32)$$

Analogously, one can cast the other expressions, such as bb^* or ab^* , into contributions including either $\omega_{j,R}$ or Γ_j . The simplification is to neglect the contributions given in terms of Γ_j , without the loss of insight or important information. This reduces all equations substantially, and under the assumption that plasma wave damping is weak, this simplification seems to be reasonable. Upon substituting the appropriate components of (31) into the auxiliary functions (23) to (25) and (28) to (30), one arrives at

$$F_{XY}^j = \frac{A^j}{k^2} [k_x k_y [(a_R k_\perp - b_R k_\parallel)^2 - b_R^2 k^2] - \imath \sigma^j b_R k_\perp^2 k (a_R k_\perp - b_R k_\parallel)] \quad (33)$$

$$F_{YX}^j = \frac{A^j}{k^2} [k_x k_y [(a_R k_\perp - b_R k_\parallel)^2 - b_R^2 k^2] + \imath \sigma^j b_R k_\perp^2 k (a_R k_\perp - b_R k_\parallel)] \quad (34)$$

$$G_{XY}^j = \frac{A^j k_\perp}{k^2} \sqrt{1 - \mu^2} [k_\perp^2 (a_R k_\perp - b_R k_\parallel) - 2\imath \sigma^j b_R k k_x k_y] \quad (35)$$

$$G_{YX}^j = \frac{A^j k_\perp}{k^2} \sqrt{1 - \mu^2} [k_\perp^2 (a_R k_\perp - b_R k_\parallel) + 2\imath \sigma^j b_R k k_x k_y] \quad (36)$$

$$H_{XY}^j = H_{YX}^j = A^j (1 - \mu^2) \frac{k_x k_y k_\perp^2}{k^2}, \quad (37)$$

where

$$a_R = \frac{n}{W} \sqrt{1 - \mu^2} - \frac{\omega_{j,R} k_\perp}{v k^2} ; \quad b_R = \frac{\omega_{j,R} k_\parallel}{v k^2} - \mu. \quad (38)$$

According to equations (22) and (27), one has to take the real part of the wavenumber integral. In view of the resonance function (26) and Eqs. (33) to (37), it is clear that further calculations involve both the real and imaginary part of equation (26). This is not the case for quasilinear perpendicular diffusion, where the real part of the resonance function (26) is required only (Stawicki 2004).

In order to proceed, equations (33) to (37) are substituted into the coefficients (22) and (27) and the relation $a_R k_\perp - b_R k_\parallel = (k_\parallel v_\parallel - \omega_{j,R} + n\Omega)/v$ is used. The coefficients D_{XY} and D_{YX} can

then be expressed as

$$\left. \begin{matrix} D_{XY} \\ D_{YX} \end{matrix} \right\} = R \sin \psi \cos \psi + \left\{ \begin{matrix} -N \\ +N \end{matrix} \right. \quad (39)$$

with the operator

$$R = \frac{v^2}{B_0^2} \sum_j \sum_{n=-\infty}^{\infty} \int d^3k \frac{\Gamma_j A^j(k_{\perp}, k_{\parallel}) k^{-2}}{\Gamma_j^2 + (k_{\parallel} v_{\parallel} - \omega_{j,R} + n\Omega)^2} \left\{ [(ak_{\perp} - bk_{\parallel})^2 - b^2 k^2] J_n^2(W) \right. \quad (40)$$

$$\left. - 2\sigma^j b k k_{\perp} \sqrt{1 - \mu^2} J_n(W) J'_n(W) - (1 - \mu^2) k_{\perp}^2 [J'_n(W)]^2 \right\}$$

representing resonant wave-particle interactions. The contribution N represents non-resonant behavior and reads

$$N = \frac{v}{B_0^2} \sum_j \sum_{n=-\infty}^{\infty} \int d^3k \frac{A^j(k_{\perp}, k_{\parallel})}{k^2} \frac{(k_{\parallel} v_{\parallel} - \omega_{j,R} + n\Omega)^2}{\Gamma_j^2 + (k_{\parallel} v_{\parallel} - \omega_{j,R} + n\Omega)^2} \times \left\{ \sigma^j \left(\frac{\omega_{j,R} k_{\parallel}}{v k^2} - \mu \right) k J_n^2(W) + \sqrt{1 - \mu^2} k_{\perp} J_n(W) J'_n(W) \right\}. \quad (41)$$

A closer inspection of the operator (40) results in the finding that $R \sin \psi \cos \psi = 0$, since no additional dependences in ψ are assumed. This implies vanishing resonant wave-particle interactions. Quasilinear particle drift is then solely characterized by the non-resonant term N , equation (41). Upon using the relation (5), one obtains

$$\kappa_{XY} = -\kappa_{YX} = -\frac{1}{2} \int_{-1}^1 d\mu N. \quad (42)$$

As expected for particle drift, κ_{XY} and κ_{YX} are antisymmetric. The nonresonant part, Eq. (41), allows to determine the drift coefficient (42) for different turbulence geometries. Motivated by theoretical work (Zank & Matthaeus 1992) and observations (Matthaeus et al. 1990; Bieber et al. 1996), slab and 2D turbulence geometries are assumed here, and each is considered in turn.

3. DRIFT COEFFICIENT FOR SLAB GEOMETRY

In slab turbulence geometry, the wavevectors are all either parallel or antiparallel to the background magnetic field, and the wave power spectrum can be given by

$$A^j = S_s^j(k_{\parallel}) \frac{\delta(k_{\perp})}{k_{\perp}}. \quad (43)$$

To calculate κ_{XY} or, simultaneously, κ_{YX} for slab geometry, the Bessel functions in equation (41) are considered in the limit $W \propto k_{\perp} \rightarrow 0$. The first term in the braces contributes only for $n = 0$,

since $J_n(0) = 1$ for $n = 0$ only. Concerning the second term, it can be shown that it vanishes completely for $W \rightarrow 0$ and all n . The pitch-angle integration is elementary and (42) then yields

$$\kappa_{XY}^S = -\frac{\pi}{B_0^2} \sum_{j=\pm 1} \int_{-\infty}^{\infty} dk_{\parallel} \sigma^j(k_{\parallel}) S_s^j(k_{\parallel}) k_{\parallel}^{-2} \left\{ 2\omega_{j,R} + \frac{\Gamma_j^2}{2vk_{\parallel}} \ln \left(\frac{\Gamma_j^2 + (k_{\parallel}v - \omega_{j,R})^2}{\Gamma_j^2 + (k_{\parallel}v + \omega_{j,R})^2} \right) \right\}, \quad (44)$$

For further process, the wave power spectrum $S_s^j(k_{\parallel}) = C(\nu) \lambda_s (\delta B_s^j)^2 (1 + k_{\parallel}^2 \lambda_s^2)^{-\nu}$ is employed. Here, λ_s is the bend-over scale, $(\delta B_s^j)^2$ is the slab variance and $2\nu = 5/3$ is the inertial range spectral index. Furthermore, $C(\nu) = (2\sqrt{\pi})^{-1} \Gamma(\nu)/\Gamma(\nu - 1/2)$, where $\Gamma(x)$ denotes the Gamma function. Concerning the plasma wave dispersion relation, it is assumed that forward ($j = +1$) and backward ($j = -1$) propagating shear Alfvén waves with real frequency $\omega_{j,R} = jv_A k_{\parallel}$ form the slab turbulence. For $v_A/v \ll 1$, the second term in equation (44) then becomes zero. This does not imply that the dynamical behavior of the turbulence due to dissipation is not taken into account, it is rather suppressed since the argument of the logarithmic expression becomes unity. Upon using a constant magnetic helicity, the wavenumber integration can be performed analytically and equation (44) yields

$$\kappa_{XY}^S = -\kappa_{YX}^S = -\kappa_0 \left[\sigma^+ \left(\frac{\delta B_S^+}{\delta B_S} \right)^2 - \sigma^- \left(\frac{\delta B_S^-}{\delta B_S} \right)^2 \right]. \quad (45)$$

Here, $\kappa_0 = \pi \xi \lambda_s v_A (\delta B/B_0)^2$, where $0 \leq \xi = \delta B_s^2/\delta B^2 \leq 1$ measures the fraction of the slab contribution to the total turbulent magnetic energy, $\delta B^2 = \delta B_s^2 + \delta B_{2D}^2$. The evaluation of Eq. (42) for 2D turbulence geometry is presented in the next section. A closer inspection of the slab drift coefficient (45) results in the following findings: First, κ_{XY}^S is entirely determined by the magnetic helicities σ^+ and σ^- of forward and backward propagating wave fields, respectively. Second, κ_{XY}^S depends on neither the charge nor the mass of the particle and is, therefore, independent of particle properties.

In view of the independence of κ_{XY}^S of particle properties, it is instructive to recall a standard zeroth-order drift, the $\mathbf{E} \times \mathbf{B}$ drift. A charged particle moves with the drift velocity $\mathbf{v}_D = c(\mathbf{E} \times \mathbf{B})/B^2$ if an electric force acts normal to the background magnetic field. This drift is identical for all charged particles and, therefore, independent of particle charge, mass and velocity. Equation (45) reveals the same feature. An enlightening approach for a comparison is to replace \mathbf{E} by the fluctuating field $\delta \mathbf{E}$. The drift velocity \mathbf{v}_D is then a random quantity and a corresponding velocity cross-correlation function and, therefore, drift coefficient can be derived. Based on this, it can be shown that κ_{XY}^S is indeed a result of the $\delta \mathbf{E} \times \mathbf{B}_0$ drift, where the perpendicular force results from the electric component of the turbulence.

To obtain some more insight into the drift coefficient (45), it is convenient to recall the definition of the magnetic helicity σ^j . It is usually defined as

$$\sigma^{\pm} = \frac{(\delta B_L^{\pm})^2 - (\delta B_R^{\pm})^2}{(\delta B_L^{\pm})^2 + (\delta B_R^{\pm})^2}, \quad (46)$$

where δB_L and δB_R denote left-handed (LHP) and right-handed polarized (RHP) field components of the fluctuations, respectively (see, e.g., Schlickeiser 2002). Now a variety of wave fields with different polarization states and propagation directions can be considered:

- (1) LHP wave in forward direction ($\sigma^+ = +1$, $\delta B_S^- = 0$): equation (45) yields $\kappa_{XY}^S = -\kappa_0$. A RHP wave in backward direction ($\sigma^- = -1$, $\delta B_S^+ = 0$) leads to the same result, i.e., a LHP wave in forward direction can be replaced by a RHP wave propagating in backward direction. If both are present, the drift becomes two times stronger, $\kappa_{XY}^S = -2\kappa_0$.
- (2) RHP wave in forward direction ($\sigma^+ = -1$, $\delta B_S^- = 0$): equation (45) yields $\kappa_{XY}^S = +\kappa_0$. A LHP wave in backward direction ($\sigma^- = +1$, $\delta B_S^+ = 0$) leads to the same result. As in case (1), if both types of waves are present, the drift becomes two times stronger, i.e., $\kappa_{XY}^S = +2\kappa_0$.
- (3) For equal polarization states, i.e., $\sigma^+ = \sigma^-$, one finds $\kappa_{XY}^S = -\kappa_0 H_c \sigma^+$ with

$$H_c = \frac{(\delta B^+)^2 - (\delta B^-)^2}{(\delta B^+)^2 + (\delta B^-)^2} \quad (47)$$

being the normalized cross helicity (Schlickeiser 2002). It represents the ratio of the intensities of forward ($j = +1$) to backward ($j = -1$) propagating wave fields and is sometimes also referred to as “Alfvénicity”. Obviously, κ_{XY}^S becomes zero for a vanishing net polarization. Furthermore, it changes sign if predominantly LHP or RHP wave fields are present, i.e., with the reversal of polarity.

At a glance, the drift coefficient for slab geometry, Eq. (45), is solely determined by the magnetic helicity σ^j and the real frequency $\omega_{j,R}$. If one of them is neglected, no QLT particle drift occurs in slab turbulence. However, Forman et al. (1974) and Bieber & Matthaeus (1997) argued that FLRW governs drift in a static and purely magnetic slab turbulence. In stark contrast to this are equations (44) and (45). They clearly show that particle drift in slab geometry requires turbulent electric field components and is due to the net polarization only, i.e., the magnetic helicity σ^j . Furthermore, the *nonresonant* FLRW limit used by Forman et al. (1974) and Bieber & Matthaeus (1997) is based on the concept of a magnetic power spectrum at zero wavenumber, $\delta B^2(k_{\parallel} = 0)$. This limit can be achieved only for static ($\Gamma_j = 0$) turbulence conditions. The *real* part of the resonance function (26) yields then a Dirac delta distribution $\delta(k_{\parallel})$ required for the FLRW limit. However, the real part represents *resonant* interactions. As it is shown in Sec. 2.3, the real part is not important for QLT particle drift, and so FLRW. QLT drift in slab geometry is a consequence of the *nonresonant* term, Eq. (41). The latter results from the *imaginary* part of equation (26) and can not explain the FLRW limit.

4. DRIFT COEFFICIENT FOR 2D GEOMETRY

Having derived the drift coefficient for a plasma wave turbulence and gained the insight that fluctuating electric fields are required for QLT drift in slab geometry, the evaluation of the non-

resonant contribution (41) for 2D geometry is presented in this section. For 2D geometry, the wavevectors are perpendicular to the mean magnetic field, and the wave power spectrum can be given by

$$A^j(k_\perp, k_\parallel) = S_{2D}^j(k_\perp) \frac{\delta(k_\parallel)}{k_\perp}. \quad (48)$$

Obviously, shear Alfvén waves as used in the previous section for slab turbulence can not contribute, since $\omega_{j,R} = 0$ in equation (41) for the power spectrum (48). The calculations are, therefore, restricted to purely dynamical magnetic fluctuations. Since the concept of a superposition of individual wave modes does not apply anymore, the j -nomenclature is dropped. The only modification concerns the resonance function (26). To take into account the dynamical behavior of purely dynamical magnetic fluctuations, Bieber et al. (1994) defined two models: the damping as well as the random sweeping model. For the damping model, they suggested a dynamical behavior of the turbulent energy being of the form

$$\langle \delta B_\alpha(\mathbf{k}, t) \delta B_\beta^*(\mathbf{k}, t + \xi) \rangle = P_{\alpha\beta}(\mathbf{k}) \exp(-\nu_c \xi), \quad (49)$$

where ν_c represents decay of turbulent magnetic energy. The resonance function (26) has to be adapted in this respect, and the plasma wave dissipation rate Γ_j is simply replaced by the decorrelation rate ν_c .

Upon substituting equation (48) into (41), replacing Γ_j by ν_c and applying the μ -average, one obtains

$$\kappa_{XY}^{2D} = -\frac{4\pi v}{B_0^2} \sum_{n=1}^{\infty} \int_0^{\infty} dk_\perp \frac{S_{2D}(k_\perp)}{k_\perp} \frac{n^2 \Omega^2}{\nu_c^2(k_\perp) + n^2 \Omega^2} \int_0^1 d\mu \sqrt{1 - \mu^2} J_n(W) J_n'(W). \quad (50)$$

Here, the fact was used that the first term in equation (41) is an odd function in μ and, therefore, vanishes, due to the μ -average. As a consequence, the magnetic helicity σ (not assumed to be zero) does not influence quasilinear drift in 2D turbulence geometry. The μ -integration in equation (50) can be carried out analytically and the detailed calculations are presented in Appendix A. There, it is shown that equation (50) can be manipulated to become

$$\kappa_{XY}^{2D} = -\kappa_{YX}^{2D} = -\frac{\pi v}{4B_0^2} R_L \int_0^{\infty} dk_\perp S_{2D}(k_\perp) I(\zeta, z) \quad (51)$$

with

$$I(\zeta, z) = \int_0^{\pi/2} d\theta \frac{\sin(2\theta) \sinh(2\theta z)}{\zeta^3 \sinh(z\pi) \cos^3 \theta} \left[2\zeta \cos \theta \cos(2\zeta \cos \theta) + (4\zeta^2 \cos^2 \theta - 1) \sin(2\zeta \cos \theta) \right], \quad (52)$$

where the abbreviations $\zeta = k_\perp R_L$ and $z = \nu_c / \Omega$ are introduced. Furthermore, $R_L = v / \Omega$ is the Larmor radius. Equation (51) is valid for a power spectrum and a decorrelation rate varying

arbitrarily in wavenumber k_{\perp} . It is noteworthy that a similar expression can also be derived for quasilinear perpendicular diffusion in 2D turbulence geometry (Stawicki 2004). The integral representation (52) results from the μ -integration and has to be evaluated for further progress. Unfortunately, an analytical solution to this integral does not exist, and any progress requires a numerical treatment. Figure 1 shows numerical computations of equation (52) as functions of $\zeta = k_{\perp} R_L$ for three different values of z . For illustrative purposes, z is assumed to be a constant in k_{\perp} . Using small argument approximations for the hyperbolic sine, it can be shown that Eq. (52) is independent of z and a function of ζ only. Furthermore, note that $I(\zeta, z)$ and, therefore, κ_{XY}^{2D} changes sign with the reversal of a positive to a negative particle charge state.

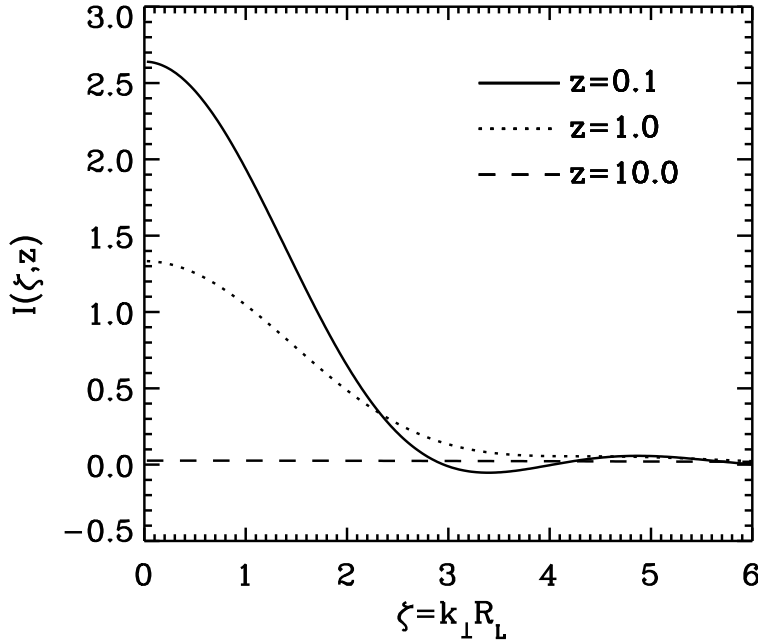


Fig. 1.— Plot of numerical solutions to Eq. (52) representing $I(\zeta, z)$ as a function of $\zeta = k_{\perp} R_L$ for three different values of z (see legend).

The limit $\zeta \ll 1$, implying $R_L \ll k_{\perp}^{-1}$, leads to an instructive, analytical solution for equation (52). To show this, small argument approximations for the circular functions are used, i.e., $\cos(2\zeta \cos \theta) \simeq 1$ and $\sin(2\zeta \cos \theta) \simeq 2\zeta \cos \theta$ and inserted into $I(\zeta, z)$. Partial integration then results in $I(\zeta \ll 1, z) = 8/3(1 + z^2)$. Consequently, one obtains for the drift coefficient the expression

$$\kappa_{XY}^{2D} = -\frac{2\pi v}{3B_0^2} R_L \int_0^{\infty} dk_{\perp} S_{2D}(k_{\perp}) \frac{(\tau_c \Omega)^2}{1 + (\tau_c \Omega)^2} \quad (53)$$

in the limit $R_L \ll k_{\perp}^{-1}$, where the relation $\nu_c = \tau_c^{-1}$ has been used. Since the correlation time τ_c is still undetermined, equation (53) can be considered as being valid regardless of whether $\tau_c \Omega$

is smaller than, larger than, or of order unity. However, in view of the restriction $k_{\perp} R_L \ll 1$, it becomes obvious that (53) is valid only for low/intermediate particle energies if parameters are assumed being typical for the heliosphere. An eye-catching feature of equation (53) is the term including the dimensionless product $\tau_c \Omega$. It is formally the same as those given in equation (3) used by Forman et al. (1974) and Bieber & Matthaeus (1997) for the FLRW limit.

5. NUMERICAL CALCULATIONS AND CONCLUSIONS

To demonstrate the potential and flexibility provided with the new drift coefficients, the remaining wavenumber integration in κ_{XY}^{2D} , Eq. (51), is solved numerically and a two-component, slab/2D turbulence is considered. Since the individual contributions are simply additive, the total drift coefficient $\kappa_F = \kappa_{XY}^S + \kappa_{XY}^{2D}$, induced by the fluctuations, is introduced, where equations (45) and (51) are used for κ_{XY}^S and κ_{XY}^{2D} , respectively. For the 2D component, the magnetic power spectrum

$$S_{2D}(k_{\perp}) = (1 - \xi) C(\nu) \lambda_{2D} \delta B^2 (1 + k_{\perp}^2 \lambda_{2D}^2)^{-\nu} \quad (54)$$

is employed. Here, as for the slab drift coefficient, $C(\nu) = (2\sqrt{\pi})^{-1} \Gamma(\nu) / \Gamma(\nu - 1/2)$ and $0 \leq \xi = \delta B_s^2 / (\delta B_s^2 + \delta B_{2D}^2) \leq 1$, where δB_{2D}^2 is the total variance of the 2D-component. The corresponding bend-over scale is given by λ_{2D} and $2\nu = 5/3$ is the inertial range spectral index. For the numerical treatment, the turbulence decorrelation rate ν_c has to be specified entering equation (51) via $z = \nu_c / \Omega$. In analogy to Bieber et al. (1994), ν_c is assumed to be of the form $\nu_c = \alpha v_A k_{\perp}$ where the parameter $0 \leq \alpha \leq 1$ allows adjustment of the strength of dynamical effects. The case $\alpha = 0$ represents the magnetostatic limit, $\alpha = 1$ describes a strongly dynamical magnetic turbulence.

For the numerical computations, conventional parameters being typical for the heliosphere are used. The ratio $(\delta B / B_0)^2$ is assumed to be 0.2, until otherwise noted. The parameter α is set to unity and the Alfvén speed v_A is chosen to be 50 km s^{-1} . The background magnetic field B_0 is given by $4 \cdot 10^{-5} \text{ Gauss}$. For all calculations, it is assumed that the turbulent magnetic energy has only a small fraction in its slab component (say 20%) and is dominated by the 2D turbulent energy (80%), yielding $\xi = 0.2$. Until noted otherwise, it is assumed that $\lambda_s = 10 \lambda_{2D} = 0.03 \text{ AU}$ (Bieber et al. 1994). For convenience, all Figures show absolute values of the drift coefficients.

Figure 2 shows numerical result of κ_{XY}^{2D} , Eq. (51), as a function of the proton Larmor radius R_L normalized to the slab bend-over scale λ_s for $\xi = 0.2$ and three different values of λ_{2D} / λ_s (see legend). The ratio R_L / λ_s is proportional to the particle rigidity R . For the computations, it is assumed that the slab contribution is unpolarized, i.e., $\sigma^+ = \sigma^- = 0$, yielding $\kappa_{XY}^S = 0$. The additional solid line visualizes the large-scale drift coefficient κ_A , Eq. (2). A closer inspection of Figure 2 results in the following finding: κ_{XY}^{2D} and κ_A obey the same power law dependence in R_L / λ_s or, alternatively, rigidity R for $R_L / \lambda_s \ll 1$, namely R^2 . This is expected. As it is shown in Sec. 4, the general 2D drift coefficient (51) reduces to equation (53) for $R_L \ll k_{\perp}^{-1}$. Obviously, κ_A and κ_{XY}^{2D} then reveal the same variation in R_L / λ_s or, synonymously, R . However, independent

of the ratio λ_{2D}/λ_s , κ_{XY}^{2D} becomes a constant for $R_L/\lambda_s \gg 1$, whereas κ_A scales with R . For completeness, Figure 3 illustrates numerical results of κ_{XY}^{2D} for protons, electrons and helium for $\lambda_{2D}/\lambda_s = 10$.

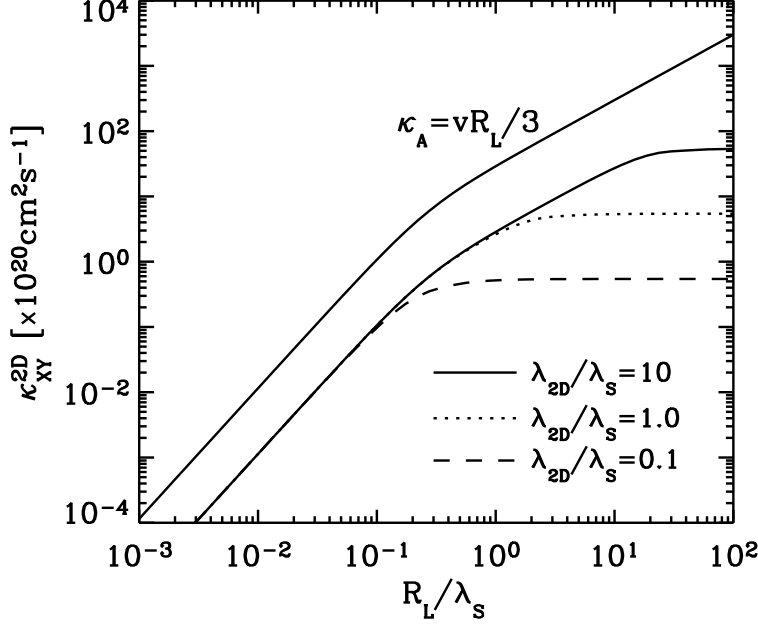


Fig. 2.— Numerical solutions to Eq. (51) representing κ_{XY}^{2D} as a function of R_L/λ_s for protons and three different values of the ratio λ_{2D}/λ_s (see legend). The slab component is suppressed by assuming an unpolarized state ($\sigma^+ = \sigma^- = 0$), and the ratio $\delta B^2/B_0^2$ is chosen to be 0.2. It is assumed that $\delta B_{2D}^2 : \delta B_s^2 = 8 : 2$. The additional solid line visualizes the standard large-scale drift coefficient κ_A , Eq. (2).

As explained in Sec. 1, κ_A is valid for an unperturbed, unmodified Parker spiral only (see Eq. (2) and the comments following it), while κ_F describes effects due to the two-component turbulence. Generally, it is expected that additional (electro)magnetic turbulent fields alter drift effects, particularly for low and intermediate particle energies. Whether with or without turbulence, particle motion is affected by curvature and gradient drift effects. The standard coefficient κ_A might therefore be considered as the limit of a more general drift coefficient for $\delta B \rightarrow 0$ for which κ_F vanishes. Since the fluctuating fields are superimposed to the heliospheric background magnetic field, it is assumed that individual drift effects induced by B_0 and δB are simply additive (at least in the local orthogonal coordinate system). This results in a total drift coefficient $\kappa_T = \kappa_A + \kappa_F$. Note that both κ_A as well as κ_{XY}^{2D} change signs with the reversal of the particle charge state. According to Eq. (51), but also equation (45) for the slab contribution, one has to take into account an additional minus sign, resulting in the difference of κ_A and κ_F . The slab contribution is independent of the particle charge state and depends solely on the polarization of slab turbulence. In this respect, the

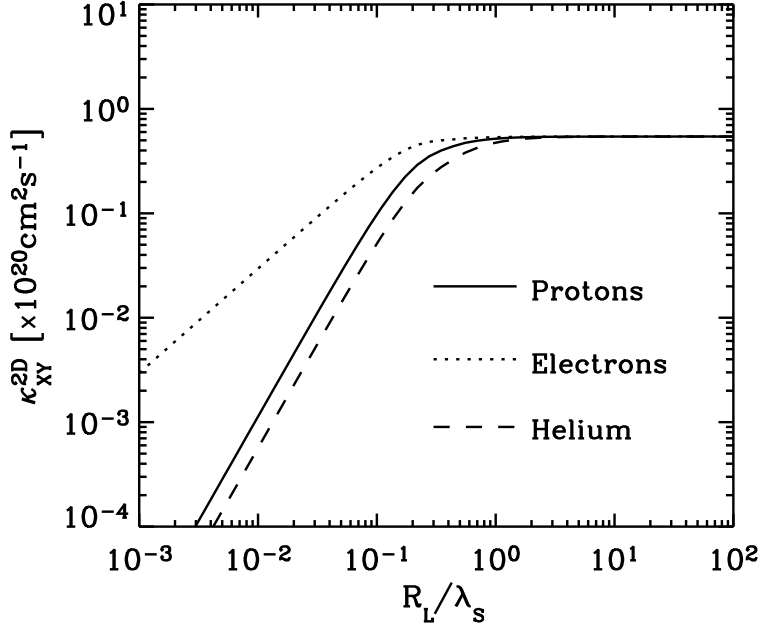


Fig. 3.— Plot of numerical solutions to Eq. (51) for $\delta B^2/B_0^2 = 0.8$, $\lambda_s = 10\lambda_{2D}$ and three different particle species: protons, electrons and helium.

magnetic helicity σ^\pm of the slab component entering equation (45) and the normalized cross helicity H_c , Eq. (47), are quite uncertain parameters. A rigorous theory describing wavenumber and radial variations of the slab helicities does not exist. Usually, for the 2D component, H_c is assumed to be zero for heliocentric distances beyond ~ 1 AU (e.g., Zank et al. 1996), but this might probably not be the case (see Matthaeus et al. 2004).

Figure 4 shows results for κ_{XY}^{2D} (solid line), κ_A (dotted line) and their difference, κ_T (dashed line), for the turbulence level $\delta B^2/B_0^2 = 0.8$ and an unpolarized slab contribution, i.e., $\kappa_{XY}^S = 0$. Here, protons are considered. At a glance, the drift coefficient κ_A is substantially reduced at low and intermediate particle rigidities. At very low rigidities, κ_T is almost two magnitudes smaller than the standard drift κ_A , but reveals the same power law behavior in rigidity, i.e., R^2 . With further increase in R , κ_T varies as $R^{7/2}$, rolling over to $\kappa_F \propto R$ at high rigidities, where the large-scale relation κ_A dominates.

As mentioned in Sec. 1, a reduction of the amount of drift effects at low and intermediate rigidities was suggested earlier by, e.g., Potgieter et al. (1987) and Burger (1990) and was then considered theoretically by Bieber & Matthaeus (1997). Assuming $\delta B^2/B_0^2 \sim 1$, Bieber & Matthaeus (1997) found a R^3 power law behavior for the scaling of drift effects at intermediate energies. However, absolutely central to their approach is the assumption that FLRW governs the reduction of the drift. This was not assumed here. The FLRW limit is rather excluded, since the *imaginary*, nonresonant part of the function (26) governs quasilinear particle drift, and not the real part.

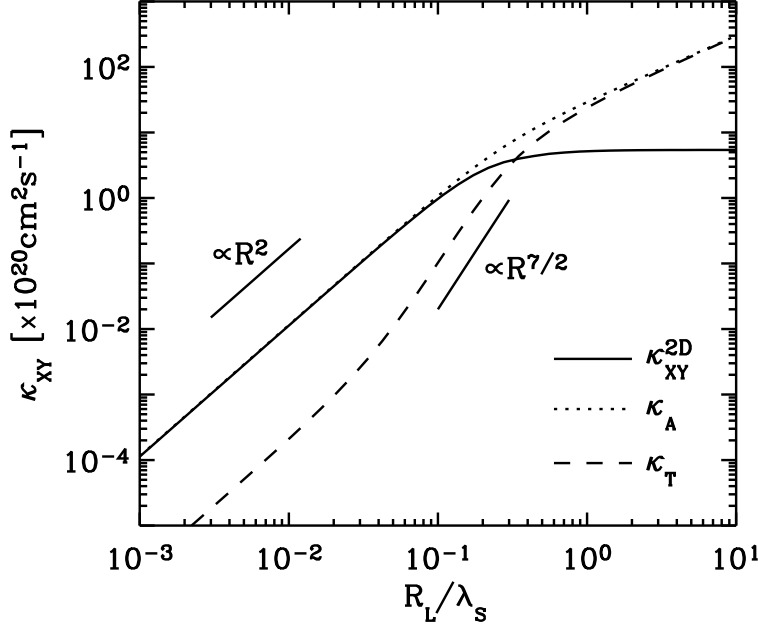


Fig. 4.— Numerical solution of κ_{XY}^{2D} (solid line) for protons and $\delta B^2/B_0^2 = 0.8$ as well as $\lambda_s = 10\lambda_{2D}$. The slab component is suppressed, $\kappa_{XY}^S = 0$, by assuming an unpolarized state, i.e., $\sigma^+ = \sigma^- = 0$. The dashed curve represents the total drift coefficient $\kappa_T = \kappa_A - \kappa_F$.

Furthermore, the argumentation by Bieber & Matthaeus (1997) is valid for slab geometry only. For the numerical computations given in Figure 4, the slab component is explicitly excluded by assuming an unpolarized state. Obviously, the reduced amount of drift effects shown in Figure 4 results rather from the presence of the 2D component than from slab turbulence and, least at all, FLRW. Depending on the ratio $\delta B^2/B_0^2$, the influence of magnetic perturbations on drift effects, induced in the local orthogonal coordinate system by curvatures and gradients of the global and unperturbed background magnetic field, leads to a significant reduction of these drift effects. The result $R^{7/2}$ for $\delta B^2/B_0^2 = 0.8$ is relatively close to the result by Bieber & Matthaeus (1997), i.e., R^3 . However, Figure 4 shows that κ_T recovers to continue with R^2 with decreasing rigidity or ratio R_L/λ_s . This is different when slab turbulence is polarized.

The influence of the slab contribution is shown in Figure 5. Here, the same linestyle and parameters are used as those for Figure 4, but a net polarization of the slab component is assumed. For this, a relatively weak right-hand polarization of forward and backward propagating wave fields is chosen, i.e., $\sigma^+ = \sigma^- = -0.1$ (see Sec. 3: item (3), page 12). For the variances of the wave fields, the ratio $(\delta B^-)^2 : (\delta B^+)^2 = 9 : 11$ is assumed, implying for the normalized cross helicity $H_c = 0.1$. This implies a slightly larger amount of turbulent energy in forward than in backward propagating wave fields. A comparison of Figures 5 and 4 results in the insight that the slab drift coefficient κ_{XY}^S becomes important only at very low values of R_L/λ_s , i.e., very low particle rigidities. For this range, κ_{XY}^S exceeds κ_{XY}^{2D} by an order of magnitude and κ_T becomes a constant for a slab component

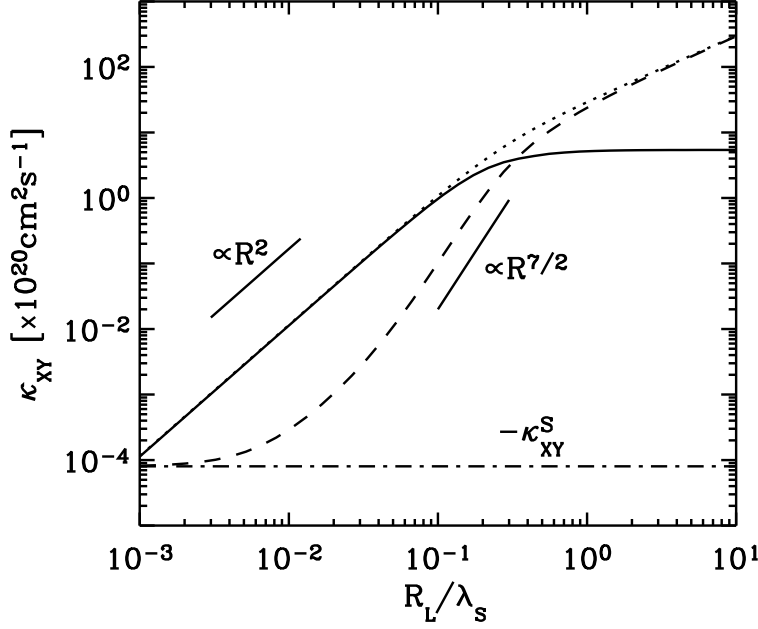


Fig. 5.— Same as Fig. 4, but the slab component is assumed to be weakly right-hand polarized ($\sigma^+ = \sigma^- = -0.1$). A slightly larger amount of turbulent energy in forward propagating wave fields is assumed, i.e. $H_c = 0.1$. The dashed-dotted curve represents $-\kappa_{XY}^S$, Eq. (45). The dashed curve represents the total drift coefficient $\kappa_T = \kappa_A - \kappa_F$.

being weakly right-hand polarized.

The reduction in the amount of drift effects and the change in rigidity dependence varies for different particle species. Figure 6 shows numerical results similar to those given in Figure 5, but now for electrons. First, as expected, the 2D drift coefficient varies as $\kappa_{XY}^{2D} \propto R$ at low and intermediate values of R_L/λ_s , indicating the relativistic nature of the electrons at such low rigidities. As a consequence of this, κ_T scales with $R^{5/2}$ instead of $R^{7/2}$ and rolls then over to $\kappa_T \propto R$ at high rigidities.

The aforementioned long-standing assumption of a vanishing normalized cross helicity h_c for heliocentric distances beyond ~ 1 AU (e.g., Zank et al. 1996) was made for the 2D turbulence component only. Unfortunately, a similar treatment for the slab component does not exist. Assuming that the same holds for slab turbulence, it implies that κ_{XY}^S vanishes in the outer heliosphere and is present only within Earth’s orbit. In this case, the 2D component dominates QLT particle drift throughout the outer heliosphere, since it does not depend on any helicity (see Eq. (50) and the comments following it). However, using a more advanced transport model including cross helicity, Matthaeus et al. (2004) recently relaxed the assumption of a vanishing cross helicity for 2D turbulence. Their study indicates that cross helicity might even be present at around 10 AU. Assuming

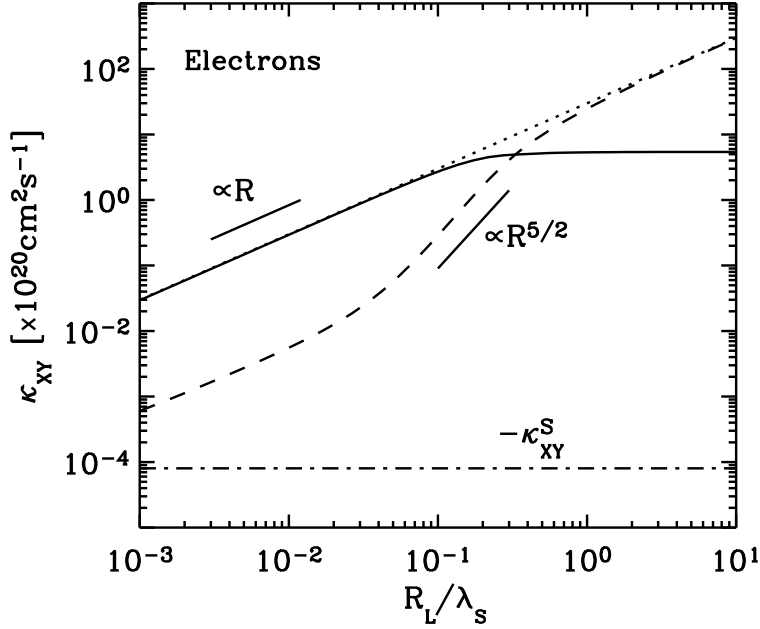


Fig. 6.— Numerical solution of κ_{XY}^{2D} (solid line) for the same parameters and linestyle as those used for the computations shown in Fig. 5, but here for electrons.

that the same statement holds for slab turbulence, this would imply that κ_{XY}^S might become important not only at Earth, but also for heliocentric distances within Jupiter’s and Saturn’s orbit, especially for low rigidity particles and provided that slab turbulence is polarized (even if weakly only).

Another very interesting issue, which can be addressed in the context of magnetic helicity and its importance for QLT particle drift in slab geometry, concerns the helicity density of the large-scale HMF. Bieber et al. (1987) have considered the topological properties of the Parker interplanetary field and have shown that the helicity density of the Parker field is negative north of the heliospheric current sheet and positive south of the current sheet, independent of the sign of the solar poloidal magnetic field. Bieber et al. (1987) argue that the magnetic helicity of interplanetary small-scale turbulence may well be related to the helicity of the large-scale Parker field. This implies here that the magnetic helicity and, therefore, the polarization state of the slab component north of the heliospheric current sheet is opposite in sign to the polarization of the slab component south of the current sheet. In view of this implication, the slab drift coefficient κ_{XY}^S , Eq. (45), would reverse sign across the heliospheric current sheet, regardless of the particle charge state. Since the 2D drift coefficient κ_{XY}^{2D} , equation (51), is independent of the magnetic helicity, only the drift coefficient for slab geometry would be affected by the change of sign across the current sheet. However, κ_{XY}^{2D} changes sign with the reversal of the particle charge state (see Sec. 4). The above conclusions would add new elements to possible influences of the magnetic helicity (polarization) on heliospheric cosmic ray transport and their solar modulation, but the investigation of their impact

on cosmic ray solar modulation is far beyond the scope of this paper.

Finally, the question arises if the heliospheric transport of the so-called pick-up ions might not be affected by, at least, a polarized slab turbulence. Effects resulting from curvature and gradient drifts and spatial diffusion are usually assumed to be small and, therefore, negligible for this low energy particle population (see Ruciński et al. 1993).

I thank R. A. Burger, J. Minnie, H. Moraal and M. S. Potgieter for valuable and inspiring discussions. Support by the South African National Research Foundation (NRF) is acknowledged.

A. DERIVATION OF THE 2D DRIFT COEFFICIENT

To derive the drift coefficient κ_{XY}^{2D} , Eq. (51), for 2D turbulence geometry, the identity

$$J_n(W)J'_n(W) = \frac{k_\perp R_L \sqrt{1-\mu^2}}{4n} [J_{n-1}^2(W) - J_{n+1}^2(W)] \quad (\text{A1})$$

is used. Equation (50) can then be cast into the form

$$\kappa_{XY}^{2D} = -\frac{\pi v R_L}{B_0^2} \int_0^\infty dk_\perp S_{2D}(k_\perp) \int_0^1 d\mu (1-\mu^2) \sum_{n=1}^\infty \frac{n}{z^2 + n^2} [J_{n-1}^2(W) - J_{n+1}^2(W)], \quad (\text{A2})$$

where $z = \nu_c/\Omega$. Employing the relations (Gradshteyn & Ryzhik 1965)

$$J_{n\pm 1}^2(W) = \frac{2}{\pi} (-1)^{n\pm 1} \int_0^{\pi/2} d\theta J_0(2W \cos \theta) \cos(2\theta[n \pm 1]), \quad (\text{A3})$$

one obtains

$$J_{n-1}^2(W) - J_{n+1}^2(W) = \frac{4}{\pi} (-1)^{n-1} \int_0^{\pi/2} d\theta J_0(2W \cos \theta) \sin(2\theta n) \sin(2\theta). \quad (\text{A4})$$

Upon substituting equation (A4) into (A2) and making use of formula (1.445.4) of Gradshteyn & Ryzhik (1965), i.e.,

$$\sum_{n=1}^\infty (-1)^{n-1} \frac{n \sin(2\theta n)}{z^2 + n^2} = \frac{\pi \sinh(2\theta z)}{2 \sinh(z\pi)}, \quad (\text{A5})$$

equation (A2) can be manipulated to become

$$\kappa_{XY} = -\frac{2\pi v}{B_0^2} R_L \int_0^\infty dk_\perp \frac{S_{2D}(k_\perp)}{\sinh(z\pi)} \int_0^{\pi/2} d\theta \sin(2\theta) \sinh(2\theta z) I_\mu(\theta, \zeta) \quad (\text{A6})$$

with

$$I_\mu(\theta, \zeta) = \int_0^1 d\mu (1 - \mu^2) J_0(2\zeta \cos \theta \sqrt{1 - \mu^2}). \quad (\text{A7})$$

Here, $W = k_\perp R_L \sqrt{1 - \mu^2} = \zeta \sqrt{1 - \mu^2}$ is used. The μ -integration can be solved analytically (Gradshteyn & Ryzhik 1965) to obtain

$$\begin{aligned} I_\mu(\theta, \zeta) &= \sqrt{\frac{\pi}{2}} \left[\frac{J_{1/2}(2\zeta \cos \theta)}{(2\zeta \cos \theta)^{1/2}} + \frac{J_{3/2}(2\zeta \cos \theta)}{(2\zeta \cos \theta)^{3/2}} \right] \\ &= \frac{2\zeta \cos \theta \cos(2\zeta \cos \theta) + (4\zeta^2 \cos^2 \theta - 1) \sin(2\zeta \cos \theta)}{8\zeta^3 \cos^3 \theta}, \end{aligned} \quad (\text{A8})$$

where $J_{\frac{1}{2}+n}(x)$ denotes spherical Bessel functions of the first kind. The drift coefficient (A6) can then be expressed as

$$\kappa_{XY} = -\frac{\pi v}{4B_0^2} R_L \int_0^\infty dk_\perp S_{2D}(k_\perp) I(\zeta, z) \quad (\text{A9})$$

with the function $I(\zeta, z)$ as defined in equation (52).

REFERENCES

- Balescu, R., Wang, H. D., & Misguich, J. H. 1985, *Phys. Plasmas*, 1, 3826
- Bieber, J. W., Evenson, P. A., & Matthaeus, W. H. 1987, *ApJ*, 315, 700
- Bieber, J. W., Matthaeus, W. H., Smith, C. W., Wanner, W., Kallenrode, M. B., & Wibberenz, G. 1994, *ApJ*, 420, 294
- Bieber, J. W., Wanner, W., & Matthaeus, W. H. 1996, *J. Geophys. Res.*, 101, 2511
- Bieber, J. W., & Matthaeus, W. H. 1997, *ApJ*, 485, 655
- Burger, R. A. 1990, in *Physics of the Outer Heliosphere*, ed. S. Grzedzielski & D. E. Page (Oxford: Pergamon Press), 179
- Burger, R. A., & Hattingh, M. 1998, *ApJ*, 505, 244
- Forman, M. A., Jokipii, J. R., & Owens, A. J. 1974, *ApJ*, 192, 535
- Gleeson, L. 1969, *Planet. Space Sci.*, 17, 31
- Gradshteyn, I. S., & Ryzhik, I. M. 1965, *Table of Integrals Series and Products* (New York: Academic Press)
- Jokipii, J. R., Levy, E. H., & Hubbard, W. H. 1977, *ApJ*, 213, 861

- Kubo, R. 1957, J. Phys. Soc. Japan, 12, 570
- Lerche, I., & Schlickeiser, R. 2001, A&A, 378, 279
- le Roux, J. A., & Fichtner, H. 1997, J. Geophys. Res., 102, 17365
- Matthaeus, W. H., Goldstein, M. L., & Roberts, D. A. 1990, J. Geophys. Res., 95, 20673
- Matthaeus, W. H., Minnie, J., Breech, B., Parhi, S., Bieber, J. W., and Oughton, S. 2004, Geophys. Res. Lett., 31, 12803
- Parker, E. N. 1958, ApJ, 128, 664
- Parker, E. N. 1965, Planet. Space Sci., 13, 9
- Potgieter, M. S., le Roux, J.A., & Burger, R. A. 1987, Proc. 20th Int. Cosmic Ray Conf. (Moscow), 3, 287
- Potgieter, M. S., le Roux, J.A., & Burger, R. A. 1989, J. Geophys. Res., 94, 2323
- Potgieter, M. S., & Burger, R. A. 1990, A&A, 233, 598
- Potgieter, M. S., le Roux, J. A., Burlaga, L. F., & McDonald, F. B. 1993, ApJ, 403, 760
- Reinecke, J. P. L., Moraal, H., & McDonald, F. B. 1993, J. Geophys. Res., 98, 9417
- Ruciński, D., Fahr, H. J., & Grzedziński, S. 1993, Planet. Space Sci., 41, 773
- Schlickeiser, R. 2002, Cosmic Ray Astrophysics (Berlin: Springer)
- Stawicki, O. 2004, A&A, submitted
- Toptygin, I. 1985, Cosmic Rays in Interplanetary Magnetic Fields, (Dordrecht: Reidel)
- Webber, W. R., Potgieter, M. S., & Burger, R. A. 1990, ApJ, 349, 634
- Zank, G. P., & Matthaeus, W. H. 1992, J. Geophys. Res., 97, 17189
- Zank, G. P., Matthaeus, W. H., & Smith, C. W. 1996, J. Geophys. Res., 101, 17093
- Zank, G. P., Matthaeus, W. H., Bieber, J. W., & Moraal, H. 1998, J. Geophys. Res., 103, 2085